

Full scale field tests for strength assessment of peat

Essais in situ en vraie grandeur pour évaluer la résistance d'une tourbe

Zwanenburg C., Van M.A.
Deltares

ABSTRACT: The costs for improving the safety of the Dutch Dike system are significant. The safety of about 40 km of dikes along the lake 'Markermeer' have to be increased according to the calculation methods based on current knowledge. However, the Markermeer dikes were already in place when the Markermeer was still part of the Zuiderzee. Water levels in the past have been higher than current design water levels. In this area, the subsoil consists mainly of peat and soft soils. The uncertainty associated with measuring the strength of soft soil (in laboratory testing) and constitutive behavior in computer models is a research issue in the safety assessment. In order to close the knowledge gap between the real dike and the small laboratory tests, full-scale field tests in the peat area have been executed. The large-scale field test, the so-called 'container tests' and intensive monitoring are executed in order to reduce the uncertainty of the strength parameters in the assessment of the stability of dikes on peat subsoil. This paper discusses results of the lab and field tests and shows how DSS tests and ball penetrometer tests correspond well to the actual strength found in the field tests.

RÉSUMÉ : L'amélioration de la sécurité du système de digues hollandaises a un coût significatif. La sécurité d'une quarantaine de km de digues le long du lac de Markermeer a été augmentée selon les méthodes de calcul basées sur nos connaissances actuelles. Cependant, les digues de Markermeer étaient déjà en place quand le lac faisait encore partie du Zuiderzee. Dans le passé, le niveau d'eau était plus haut que celui adopté dans les calculs faits à présent. En ce lieu, le sous-sol est constitué principalement de tourbe et de sols compressibles. L'incertitude associée à la mesure de la résistance de sols compressibles (en laboratoire) et aux lois de comportement dans les modèles numériques est le sujet de recherche dans le cadre de l'évaluation de la sécurité des digues. De façon à combler l'écart entre une digue réelle et les petits essais en laboratoire, des essais à échelle réelle ont été conduits dans une zone tourbeuse. L'essai in situ en vraie grandeur, appelé « essai au conteneur » a été exécuté et un système de surveillance intensive a été mis en place de façon à réduire l'incertitude sur les paramètres de résistance dans l'évaluation de la stabilité des digues construites sur les sols tourbeux. Le papier discute les essais en laboratoire et sur le terrain et montre que les résultats des essais de cisaillement simple direct et les essais au pénétromètre à balle correspondent bien à la résistance observée lors des essais in situ.

KEYWORDS: dike technology, peat, field tests

1 INTRODUCTION

Despite the fact that for centuries dikes have been built along rivers and lakes on soft ground, the stability assessment of these structures is still inaccurate. Due to uncertainties in sub soil behaviour and the daily practice of engineers making safe estimates of each not well known parameter, low factors of safety are calculated for dikes that have functioned properly for many years or even centuries. One of these examples is the dike between Amsterdam and Hoorn, approximately 30 km north of Amsterdam, along lake Markermeer. The dike originates from medieval times and its last reinforcement was made in 1926. Since the closure of the Zuiderzee, now known as IJsselmeer and Markermeer, occurrence of extreme high water levels is strongly reduced. As a consequence, present day design water levels are lower, but consist of a longer duration than occurred in the past. Despite the history of this dike, calculations show a low stability factor and indicate dike reinforcement. The design of the required reinforcement incorporates large stability berms with lengths up to 30 m. Such reinforcement has a strong impact on the villages and small towns along this dike section.

The calculated large stability berms followed from uncertainty in the peat characteristics. Laboratory tests on peat samples are difficult to interpret and result in a large scatter. To optimize the design, a series of field tests is conducted. The aim of these field tests is to make a comparison between the strength found in the field to the laboratory test results.

2 CHARACTERIZATION OF THE PEAT SUBSOIL

Figure 1 shows the subsoil profile. The depths in this profile are related to the reference datum NAP which is approximately main sea level. The ground level is approximately NAP -1.4 m. On top a thin clayey layer is found with a thickness of 0.2 to 0.5 m, followed by a peat deposit of approximately 4.5 m, a deposit of several clay layers with a thickness of 4.5 m, a thin basal peat layer and finally a thick pleistocene sand deposit. The water table is nearly at ground level, NAP -1.5 m to -1.6m.

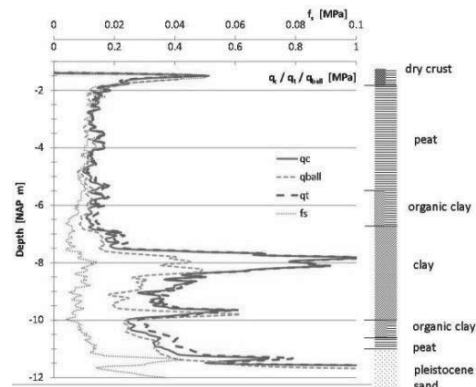


Figure 1. Typical CPT, ball penetrometer test and soil profile

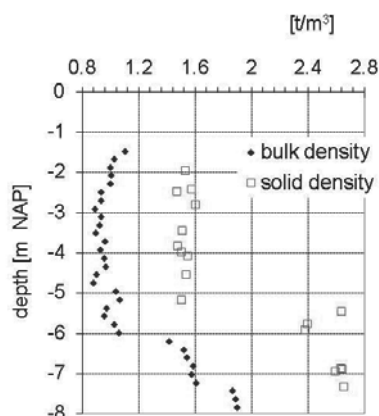


Figure 2. Bulk density and solid density, transition between peat and clay is found at NAP -5.5 m.

The peat layer is characterized as mainly sedge- reed peat. According to the von Post classification it is described as H2-H3, which means that the peat is only slightly decomposed. Figures 2, 3 and 4 give geotechnical characterisations of the peat layer.

Figure 2 shows the bulk density ρ and solid density ρ_s . For the peat samples $\rho = 0.98 \pm 0.08 \text{ t/m}^3$, while for the clay layer the bulk density increases to $\rho = 1.8 \text{ t/m}^3$ at a depth of NAP -8.5 m. Note that the peat bulk density is close to or even lower than the density of water. This can be explained by the large water content, the possible presence of gas in the peat samples and problems with re-saturating large pores in the laboratory before the bulk density measurement. The density of the solid particles, ρ_s is found by pycnometer measurements. The measurements on peat samples give $\rho_s = 1.52 \pm 0.04 \text{ t/m}^3$ while for clay samples is found $\rho_s = 2.56 \pm 0.12 \text{ t/m}^3$. The increase in bulk density at a depth of NAP -5.5 m gives a clear separation between the peat layer above NAP -5.5 m and the clay layers below.

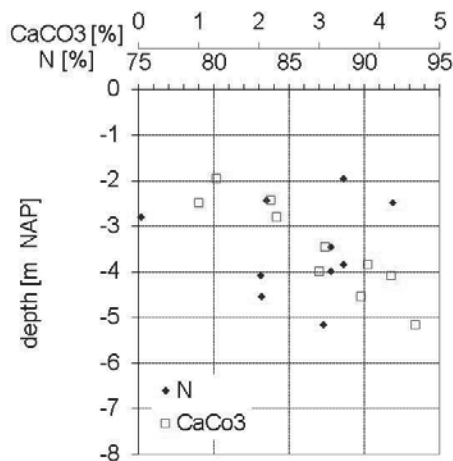


Figure 3. Loss on ignition, N and CaCO₃ content in peat layer

Figure 3 shows the loss on ignition N to be in the range of 75 to 90 % with an average value of $N = 85.7 \%$, showing the high organic nature of the peat.

To check the validity of the data, ρ_s is calculated from N following the relation given by Skempton & Petley (1970):

$$\frac{1}{\rho_s} = \frac{1 - 1.04(1 - N)}{1.4} + \frac{1.04(1 - N)}{2.7} \quad (1)$$

Equation (1) gives for $N = 0.857 [-]$, $\rho_s = 1.51 \text{ [t/m}^3]$ which is in good agreement with the measurements, $\rho_s = 1.52 \pm 0.04 \text{ [t/m}^3]$.

Samples from two borings were selected at 0.5 m depth interval for oedometer testing, provide a profile of the pre-consolidation stress and water content with depth. Besides the series of oedometer tests a number of constant rate of strain tests, so-called CRS-tests are conducted. Figure 4 shows the pre-consolidation stress found by the oedometer and CRS tests. For the oedometer tests, the pre-consolidation stress is derived according to Becker (1987), for the CRS tests the procedure according to Den Haan (2007) is applied. The profile, presented in Figure 4, shows relatively high pre-consolidation stresses in the top layer, followed by lower values in the peat layer and organic clay layer. In the non-organic clay layer the pre-consolidation stress is larger than in the peat layer. There is a clear difference in the pre-consolidation stress at the top and lower part of the peat layer. For the oedometer tests the average pre consolidation stress in the range of NAP -2.4 m to NAP -4.0 m is 10.0 kN/m^2 , with a maximum value of 13.4 kN/m^2 and a minimum value of 4.9 kN/m^2 . For the lower part an average value of 7.5 kN/m^2 is found with a maximum value of 10.6 kN/m^2 and a minimum value of 5.0 kN/m^2 . The same trend is found for the CRS tests.

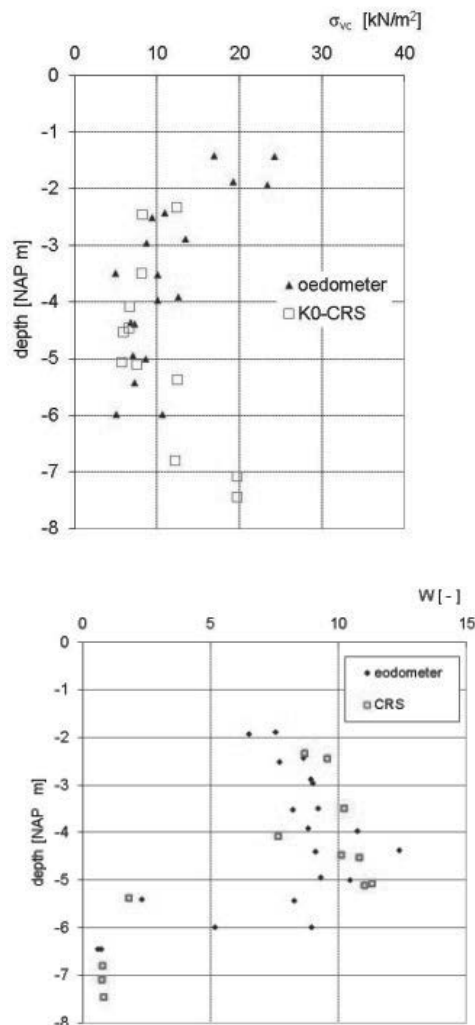


Figure 4. Oedometer and CRS test results, top: pre-consolidation stress, bottom: initial water content.

Figure 4 shows the profile of water content, defined as the mass of the pore fluid divided by the solid mass, with depth. The water content is measured before the execution of the oedometer and CRS tests. Note that the water content is given in

absolute values and not expressed as a percentage. The average water content in the peat increases with depth from 6.45 (645%) to 12.4 (1240%). The organic clay layer shows lower values, with a large scatter. In the non-organic clay layer the water content reduces to 0.74 (74%).

A series of CPTs, including measurements with different cone types and ball penetrometer tests, finalises the subsoil characterisation. Figure 1 shows a typical CPT for the test field. In this CPT, the succession of subsoil layers can be recognized. According to Eurocode ISO/DIS 22476-1:2005, IDT the measurements represent a class 2 type CPT. For a class 2 CPT the accuracy of the tip resistance, q_c , equals 100 kPa. Figure 1 indicates for the peat a tip resistance of the same order of magnitude as the accuracy for which the CPT is conducted. This is typical for peat areas and also reported for other locations Den Haan & Kruse (2007) and Boylan et al. (2011). The low accuracy for these measurements makes the conventional class 2 CPT inadequate for accurate correlations with strength parameters. Ball penetrometer tests give a more accurate reading of the resistance in peat and are therefore used for correlation purposes.

3 LABORATORY TESTING

A large series of triaxial tests and Direct Simple Shear (DSS) tests were conducted. Discussion of all the test results is beyond the scope of this paper. This paper focusses on the DSS tests for which the sample was consolidated at approximately field stresses. The results of these tests were used to correlate the undrained shear strength, s_u , to ball penetrometer tests according to equation (2).

$$s_u = \frac{q_{ball}}{N_{ball}} \quad (2)$$

in which q_{ball} represents the penetration resistance of the ball and N_{ball} represents the resistance factor.

In total 5 samples were tests at field stress conditions. Since the density of the peat is low and the water table reaches the surface the vertical effective stresses are also low, in the order of 2 – 7 kN/m². In the set-up of the field measurements for each boring, used to retrieve samples for DSS testing, a ball penetrometer test is executed at a distance of approximately 0.5 m. The DSS-strength is defined as the deflection point in the $\tau - \sigma'$ diagram, representing the shear stress where the sample behaviour changes from compression to dilation. For each sample the DSS-strength is compared to the measured resistance in the nearby ball penetrometer test at the same depth. This led to the correlation of $N_{ball} = 17.9 \pm 1.2$.

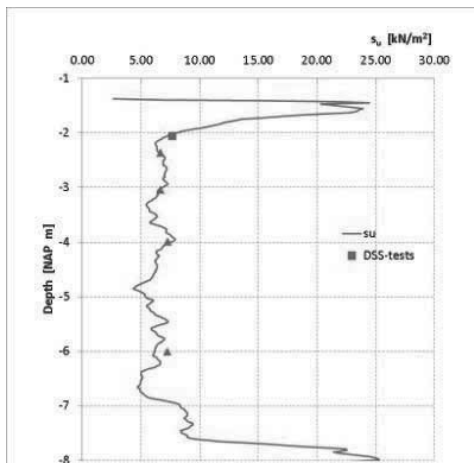


Figure 6. s_u from ball penetrometer test S15e and DSS test results. Red square indicates DSS test at nearby location, red triangles other test results.

The undrained shear strength from the DSS tests ranges from 6.7 tot 7.7 kN/m² with an average value of 7.1 kN/m². The variation in the test results is small and the average value for N_{ball} found for the individual DSS test results fits well to the overall strength profile.

4 TEST SET-UP

In total 5 field tests are conducted. In the first two tests the peat is loaded in a few days to failure. The other 3 field tests include a two-periods loading procedure with several weeks of preloading before failure. This paper focusses only on the first two tests. For testing reproducibility the test loading is identical. Figure 7 shows the 3 loading phases of these tests.

In loading phase 1, a row of containers is placed and a ditch is excavated. The containers have the dimensions of 7.25 m (length) \times 2.5 m (width) \times 2.2 m (height). The ditch has a depth of 2.5 m and slope 1:1. After excavation, the ditch bottom rose due to swelling of the peat. The remaining depth during the test was approximately 2 m.

In loading phase 2, the containers were stepwise filled with water. Each load step consisted of a 0.25 m increase in water level. It was decided to start the next step if no failure had occurred in the previous step and deformation rates slowed down significantly.

In loading phase 3, the water level in the ditch was stepwise decreased. Each step consists of a 0.25 m lowering of the water table. Failure was found after lowering the water table in loading phase 3.

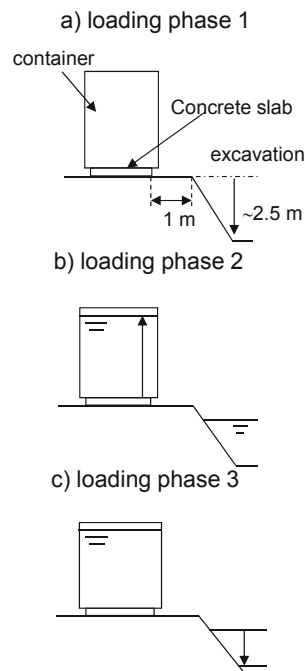


Figure 7. Planned test set-up

The instrumentation was concentrated in three measurement rows, see Figure 8. In figure 9 the location of the instrumentation placed in the second measurement row is shown. At three depths in the peat layer and at one depth in the clay layer, the pore pressure development was measured with Vibrated Wire Probes, VWP's and horizontal displacements were measured with a SAA unit, see Abdoun (2007), placed at the front of the container row. For measurement rows 1 and 2 the pore pressure development was measured at only two locations in the peat layer. Besides the instrumentation in the measurement rows the settlement under the middle two containers was measured with automated settlement plates, the water level in the container was measured for each container and the heave of the ditch after excavation was measurement with settlement plates.

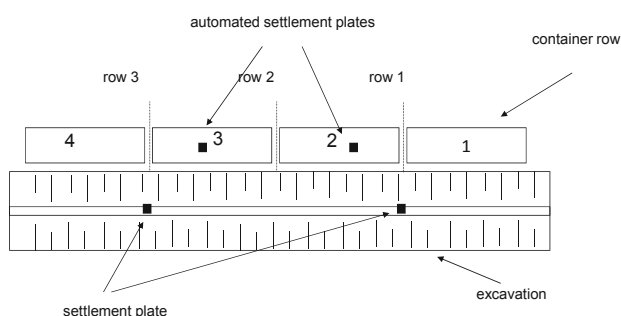


Figure 8. Top view

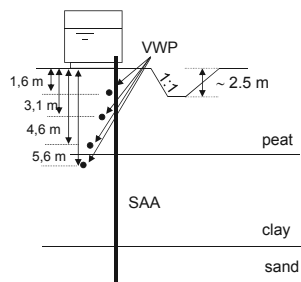


Figure 9. Instrumented cross section, VWP = vibrated wire probe.

5 RESULTS

The tests were run in approximately three days and this loading scheme resembles the loading velocity for river dikes, where high water levels rise and decline in a matter of days.

After the test was finished an excavation pit was made to study subsoil cracks and failure planes. These observations resulted in a reconstruction of the failure mechanism as shown in Figure 10. At the active side a clear and nearly vertical rupture plane was found accompanied with a secondary, backward running crack. This rupture plane intersected a nearly horizontal rupture plane. The horizontal rupture plane is only found at the active side of the failure. The maximum displacement found at the end of the test, measured at the front of the container row, is found at the same depth as the rupture plane was found at the active side. At the end of the test the slope of the ditch was nearly unaffected. This led to the conclusion that the horizontal displacements, measured at the front of the containers were followed by horizontal compaction of the peat between the containers and ditch.

Between the containers and horizontal rupture plane a series of minor horizontal and vertical cracks were found. It is not known whether these cracks were formed during the test, when the peat layer was loaded or after during swelling due to the removal of the load.

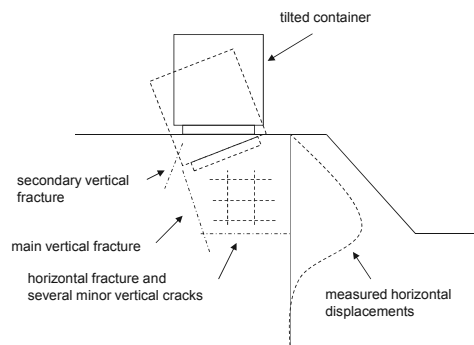


Figure 10. Sketch of failure mechanism.

6 ANALYSIS

After finalizing the field tests, an extended analysis was conducted including limit equilibrium analysis. Since the dimensions of the field tests are limited, 3D effects play a role.

Based on the dimensions of the failure planes it is estimated that the friction along the sides of the failure mechanism adds approximately 10% extra friction to a plane strain assumed failure plane. So, failure is to be found for a calculated Safety Factor, $SF = 0.9$. For the analysis the Spencer and LiftVan method were applied. The LiftVan method, Van et al (2005), is a Bishop based method and includes a horizontal sliding plane between the active and passive parts of the slip circle with different radii. Back analysis with the conditions at which failure was found led to the average undrained shear strength, s_u , available at failure. Table 1 shows the results.

 Table 1. Back analysis of test results, s_u in $[kN/m^2]$ for which $SF = 0.9$.

Model	Test 1	Test 2
LiftVan	7.0	7.8
Spencer	7.3	8.0

7 CONCLUSIONS

The large scale field tests on the peat subsoil were conducted successfully. Measurements show an equivalent development of deformations and pore pressure in both tests. Together with the small differences found in the back analysis this indicates a good reproducibility of these tests.

The strength found in the DSS lab tests, in which the samples are consolidated at field stress level, correlate well to ball penetrometer tests. This resulted in a correlation between the ball cone field test and the DSS lab test.

The back analysis of the container tests shows that the average available shear resistance during the test is in the range of 7 to 8 kN/m^2 . This corresponds well to the strength found from the DSS tests.

The combination of ball penetrometer tests and DSS tests, for which the sample is consolidated at field stress level, provide a valuable tool in obtaining peat strength parameters for safety assessments of dikes on peaty subsoil.

8 ACKNOWLEDGEMENTS

The research project, including the field tests, is initiated and funded by Hoogheemraadschap Hollands Noorderkwartier in cooperation with Rijkswaterstaat – Waterdienst.

9 REFERENCES

- Abdoun T., Bennet V., Danisch L., Shantz T. & Jang D. 2007 Field Installation details of a wire-less shape-acceleration array system for geotechnical applications *Proceedings of SPIE, San Diego* volume 6529
- Becker D.E., Crooks J.H.A., Been K., Jefferies M.G. 1987 Work as a criterion for determining in situ and yield stress in clays *Can. Geot. J* **24**:549-564
- Boylan N., Long M., Mathijssen F.A.J.M. 2011 In situ strength characterisation of peat and organic soil using full flow penetrometers *Can Geotech J.* **48**:1085-1099
- Den Haan E.J. (2007) De intrinsieke tijd in het isotachenmodel *Geotechniek* **12**(1), 34-38 (in Dutch)
- Den Haan, E.J. & Kruse, G.A.M. (2007) Characterisation and engineering properties of Dutch peats In: *Second international workshop on characterisation and engineering of natural soils Singapore* vol. 3 London Taylor & Francis p 2101 -2133
- Skempton A.W., Petley D.J. 1970. Ignition loss and other properties of peats and clays from Avonmouth, Kings Lynn and Cranberry Moss, *Geotechnique* **20** (4), 343-356.
- Van M.A., Koelewijn A.R., Barends F.B.J. 2005 Uplift phenomenon : Model, Validation and Design *international Journal of Geomechanics* **5**:2, 98-106.